Supporting Information

A Copper(I) Thiocyanate based Photoresponsive Semiconducting 2D Coordination Polymer

Tomoki Nishiyama,[a] Hirotaka Kitho-Nishioka,[b] Senku Tanaka,[b,c] Masahiko Maekawa,[a,c] Takayoshi Kuroda-Sowa,[a] Masaki Yoshida,[d] Masako Kato,[d] and Takashi Okubo*[b,c]

[a] *Department of Chemistry, Kindai University, 3-4-1 Kowakae, Higashi-Osaka, Osaka 577-5402 Japan*
[b] *Department of Energy and Materials, Kindai University, 3-4-1 Kowakae, Higashi-Osaka, Osaka 577-5402 Japan*
[c] *Research Institute for Science and Technology, Kindai University, 3-4-1 Kowakae, Higashi-Osaka, Osaka 577-5402 Japan*
[d] *Department of Applied Chemistry for Environment, School of Biological and Environmental Sciences, Kwansei Gakuin University, 1 Gakuen Uegahara, Sanda, Hyogo 669-1330, Japan.*

Materials.

The reagents were purchased from Tokyo Kasei Kogyo Co., Ltd., and Aldrich Chemical Co., Inc. All the chemicals were used without further purification. The purity of Au deposited was 99.99%.

Synthesis of $[Cu(SCN)(iqi)]_n$.

A 50 mL acetonitrile of CuSCN(I) (12.1 mg, 0.1 mmol) was stirred for 10 min and then was filtrated. The filtrate was added isoquinoline (0.0585 mL, 0.5 mmol) and stirred for 1 minute. The reaction mixture was filtrated, and yellow single crystals suitable for X-ray diffraction were obtained from the mixture in 1 day by recrystallization at ambient temperature.

Anal. Calcd for $[Cu(SCN)(iqi)]_n$ ($C_{10}H_7N_2S_1Cu_1$) ; C, 47.89; N, 11.17;H 2.81

Found ; C, 47.79 ;N, 11.18 ;H, 2.83

X-ray structure determination.

Experimental

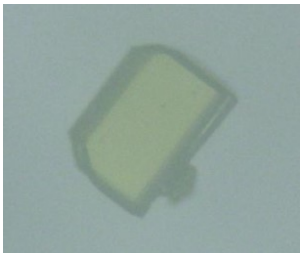

Fig. S1 Single crystal of [Cu(SCN)(iqi)]$_n$

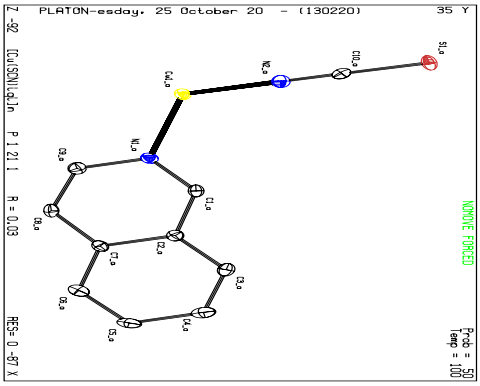

Fig S2. The ORTEP diagram of [Cu(SCN)(iqi)]$_n$

A clear light yellow block crystal of [Cu(SCN)(iqi)]$_n$ was mounted with a loop cappilary for the single crystal X-ray diffraction measurement. All measurements were made on a XtaLAB AFC12 (RINC): Kappa single diffractometer using graphite monochromated Mo-Kα radiation. The data were collected at a temperature of -173 $\pm$ 1°C to a maximum 2θ value of 62.4°. A sweep of data was done using ω scans from -89.0 to 14.0° in 0.50° step, at χ = -38.0° and ϕ = 60.0°. A second sweep was performed using ω scans from -20.0 to 8.0° in 0.50° step, at χ = 57.0° and ϕ = 150.0°. A third sweep of data was done using ω scans from 56.0 to 82.0° in 0.50° step, at χ = 57.0° and ϕ = 150.0°. A fourth sweep was performed using ω scans from -9.00 to 18.0° in 0.50° step, at χ = 77.0° and ϕ = 90.0°. A fifth sweep of data was done using ω scans from -86.0 to -23.0° in 0.50° step, at χ = - 19.0° and ϕ = 150.0°. Of the 5653 reflections were collected, where 2617 were unique (R_{int} = 0.0454). Data were collected and processed using CrysAlisPro (Rigaku Oxford Diffraction).[1] No decay correction was applied. The linear absorption coefficient (μ) for Mo-Kα radiation is 50.230 cm^{-1}. An empirical absorption correction was applied which resulted in transmission factors ranging from 0.686 to 1.000. The data were corrected for Lorentz and polarization effects. All calculations were performed using the Olex2,[2] the structure was solved with the SHELXT[3] structure solution program using Intrinsic Phasing and refined with the SHELXL[4] refinement package using Least Squares minimization. CCDC-2243630 for [Cu(SCN)(iqi)]$_n$ contains the supplementary crystallographic data for this paper.

Table 1 Crystal data and structure refinement for $[Cu(SCN)(iqi)]_n$. (**CCDC 2243630**)

Identification code	$[Cu(SCN)(iqi)]_n$
Empirical formula	$C_{10}H_7N_2SCu$
Formula weight	250.78
Temperature/K	100.15
Crystal system	monoclinic
Space group	$P2_1$
	a = 5.8691(3) Å
	b = 7.3775(4) Å
	c = 11.0578(7) Å
	β = 102.454(6) º
Volume	467.53(5) Å^3
Z	2
ρ_{calc}	1.781 g/cm^3
μ	2.511 mm^{-1}
F(000)	252.0
Crystal size	0.38 mm × 0.24 mm × 0.15 mm
Radiation	MoKα (λ = 0.71073)
2θ range for data collection	6.688 ° to 62.448 °
Index ranges	$-8 \le h \le 8$, $-10 \le k \le 10$, $-15 \le l \le 16$
Reflections collected	5653
Independent reflections	2617 [R_{int} = 0.0454, R_{sigma} = 0.0621]
Data/restraints/parameters	2617/1/127
Goodness-of-fit on F2	1.038
Final R indexes [$I > 2\sigma(I)$]	R_1 = 0.0312, wR_2 = 0.0740
Final R indexes [all data]	R_1 = 0.0329, wR_2 = 0.0751
Maximum peak in Final Diff. Map	0.41 e$^-$/Å^3
Minimum peak in Final Diff. Map	-0.45 e$^-$/Å^3
Flack parameter	-0.003(13)

Physical measurements.

UV-vis spectra were monitored on a U-4100 UV/VIS/NIR spectrophotometer (HITACHI). DC conductivity at room temperature was measured with a KEITHLY 2400 source meter. For luminescence measurement, an AvaLight-HPLED-385 LED light source from Avantes Co. was used as the excitation, and an AvaSpec-ULS2048CL-EVO-VA-50 spectrometer from Avantes Co. Gold of electrode was deposited by SVC-700TM SG (SANYUELECTRO Co.). X-ray powder diffraction was monitored on a MiniFlexII (Rigaku Co.) at room temperature. UPS measurements were monitored on PHI Versaprobe 4 by ULVAC-PHI. Inc.

PXRD of $[Cu(SCN)(iqi)]_n$

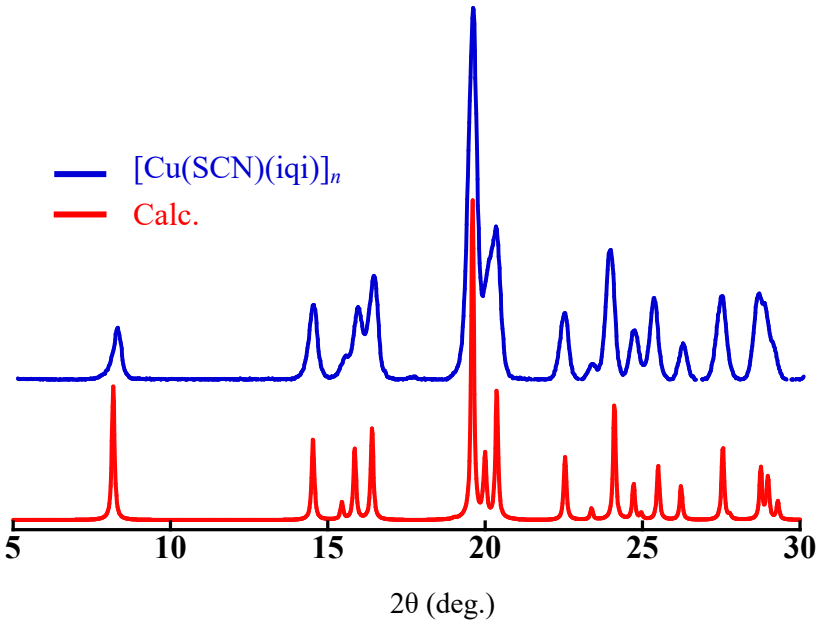

Fig. S3 Comparison of PXRD of as-synthesized $[Cu(SCN)(iqi)]_n$ and calculated ones from the single-crystal data of $[Cu(SCN)(iqi)]_n$.

Diffuse-reflectance spectra of [Cu(SCN)(iqi)] and isoquinoline

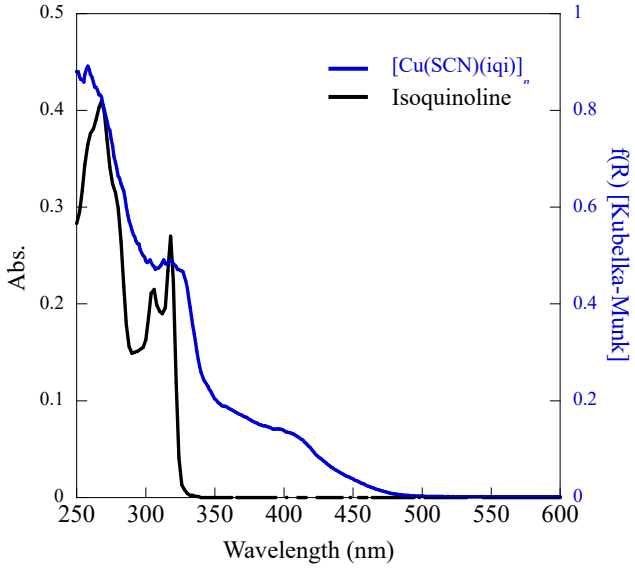

Fig. S4 (a) Diffuse-reflectance spectrum of $[Cu(SCN)(iqi)]_n$ (blue line) and absorption spectrum of iqi in a $CHCl_3$ solution (black line).

Fig. S4 shows the diffuse-reflectance spectra of $[Cu(SCN)(iqi)]_n$ doped in MgO powder (blue line) and the absorption spectra of a ligand, iqi, in a $CHCl_3$ solution (black line). The absorption of $[Cu(SCN)(iqi)]_n$ around 200 nm to 350 nm is consistent with the peaks of the ligand iqi, suggesting that the absorption is due to the π-π* transition of iqi. The absorption around 350 nm to 450 nm is attributed to MLCT from the d-orbital of Cu(I) ion to the π* orbital of iqi ligand.

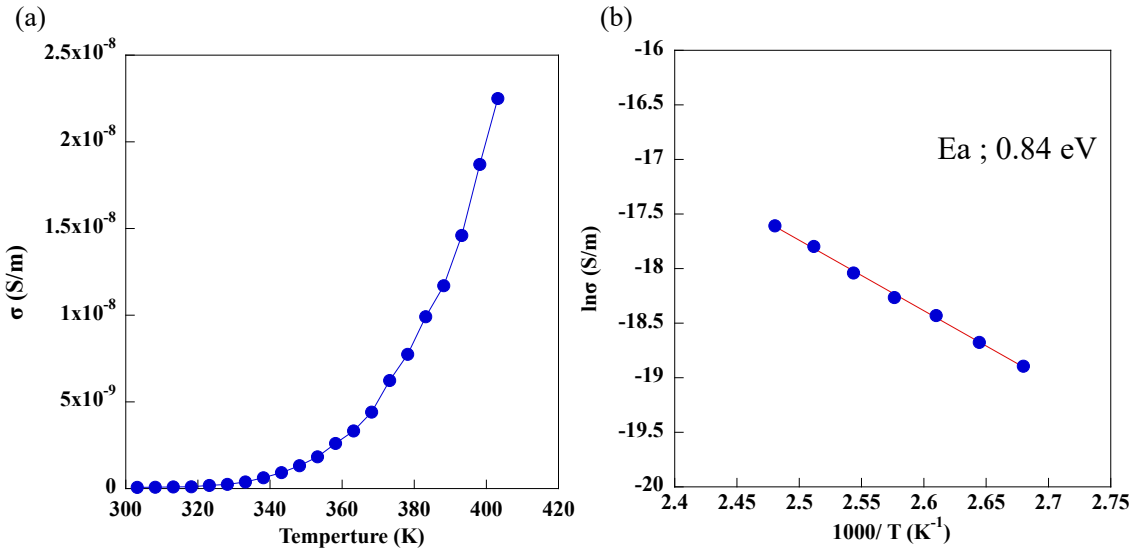

Fig. S5 (a) Temperature dependence on electrical conductivity with a pellet sample (b) Arrhenius plot of σ (bulk)

Temperture Dependence of electrical conductivity and Arrhenius plot

Table 2 Comparison of semiconductive coordination polymers.

Compounds	Conductivity / S cm^{-1}	Ref.
$[Cu(SCN)(pyridine\text{-}3,4\text{-}dicarbonitrile)_2]_n$	4.3×10^{-5}	5
$[Cu_2Br(IN)_2]_n$	1.2×10^{-5}	6
$[Cu(DPNDI)_2]_n$	1.2×10^{-5}	10
$[Cu(SCN)(py\text{-}TTF\text{-}py)]_n$	1.93×10^{-6}	7
$[Cu_2(SCN)_2(py\text{-}TTF\text{-}py)]_n$	4.50×10^{-7}	7
$[Cu_2Br_2(ttz)]_n$	8.17×10^{-10}	8
$[Cu(SCN)(iqi)]_n$	1.25×10^{-12}	this work
$[Cu(SCN)(4\text{-}cyanopyridine)_2]_n$	10^{-13}	5
$[Cu(1,2,3\text{-}triazolate)_2]_n$	3.2×10^{-14}	9
$[Cu_2(DOBDC)(DMF)_2]_n$	1.4×10^{-14}	9
$[CuBr(pyz)]_n$	8.30×10^{-16}	8

IN; isonicotinato, DPNDI; *N*,*N*'-di(4-pyridyl)-1,4,5,8-naphthalenetetra-carboxydiimide, py-TTF-py; 2,6-bis(4′-pyridyl)-tetrathiafulvalene, ttz; 1,2,4,5-tetrazine, DOBDC; 2,5-dihydrylbenzene-1,4-carboxylic acid, pyz; pyrazine

UPS measurement of [Cu(SCN)(iqi)]$_n$

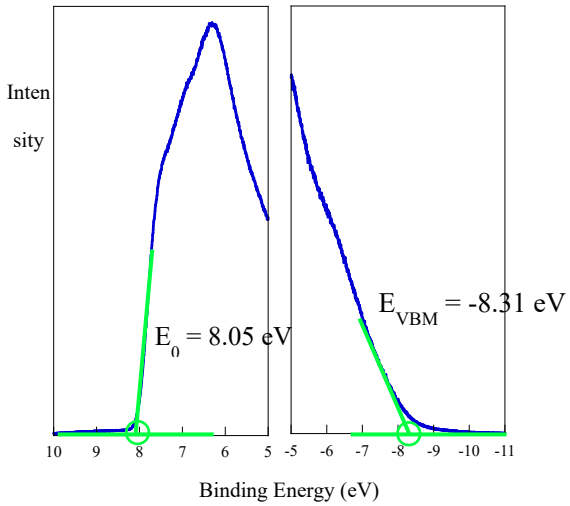

Fig. S6 UPS measurement of [Cu(SCN)(iqi)]$_n$

E_0 and E_{VBM} correspond to the intersection of the baseline along the binding energy axis and the line extrapolating the linear portion of the threshold from the UPS results (Fig. S6):

$$IP = h\nu - (E_0 - E_{VBM})$$

where hν is 21.2 eV of the He(I) line, and IP, E_0 and E_{VBM} are the ionization potential, cut off energy and upper end of the valence band, respectively.

Luminescence of [Cu(SCN)(iqi)]$_n$

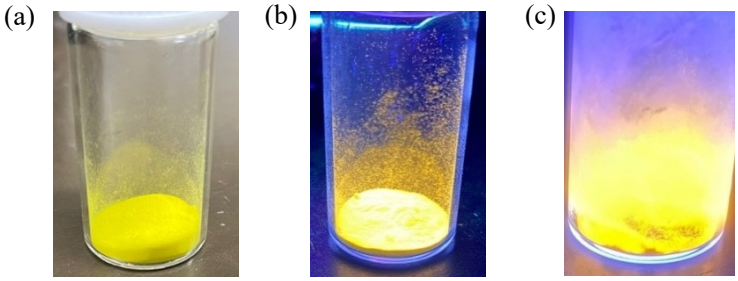

Fig. S7 Sample pictures of [Cu(SCN)(iqi)]$_n$ at r.t. (a), under UV-light irradiation at r.t. (b), and under UV-light irradiation at 77K (c).

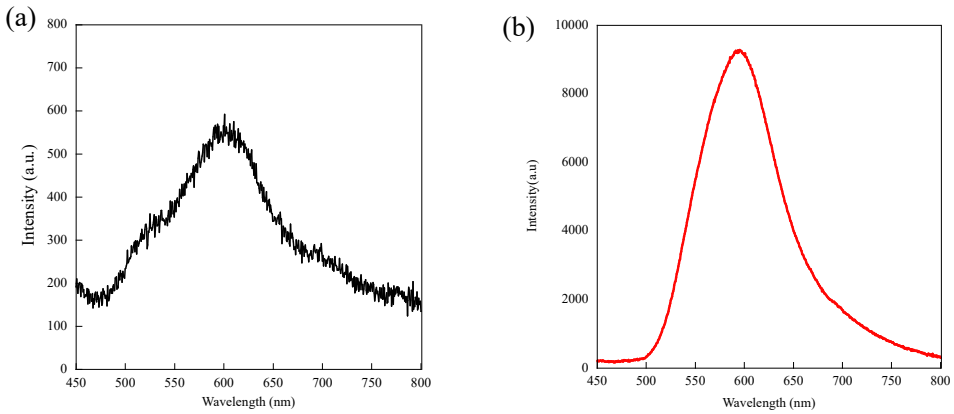

Fig. S8 Luminescence spectra of $[Cu(SCN)(iqi)]_n$ excited at 385 nm at r.t. (a) and 77 K (b).

Emission Decay behavior of $[Cu(SCN)(iqi)]_n$

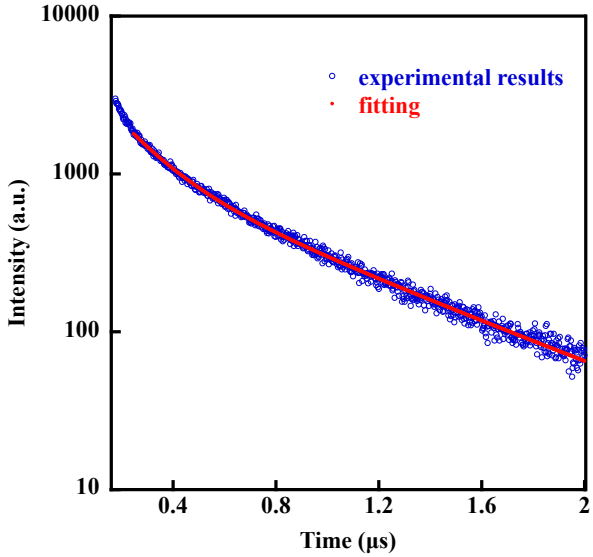

Fig. S9 PL decay behavior of $[Cu(SCN)(iqi)]_n$ at room temperature.

Table 3 Fitting parameters for the emission decay curve of $[Cu(SCN)(iqi)]_n$ at room temperature.

Compound	A_1	τ_1 (μs)	A_2	τ_2 (μs)	$\tau_{ave.}$ (μs)	R_2
$[Cu(SCN)(iqi)]_n$	0.494	0.169	0.506	0.650	0.552	1.07

K-path

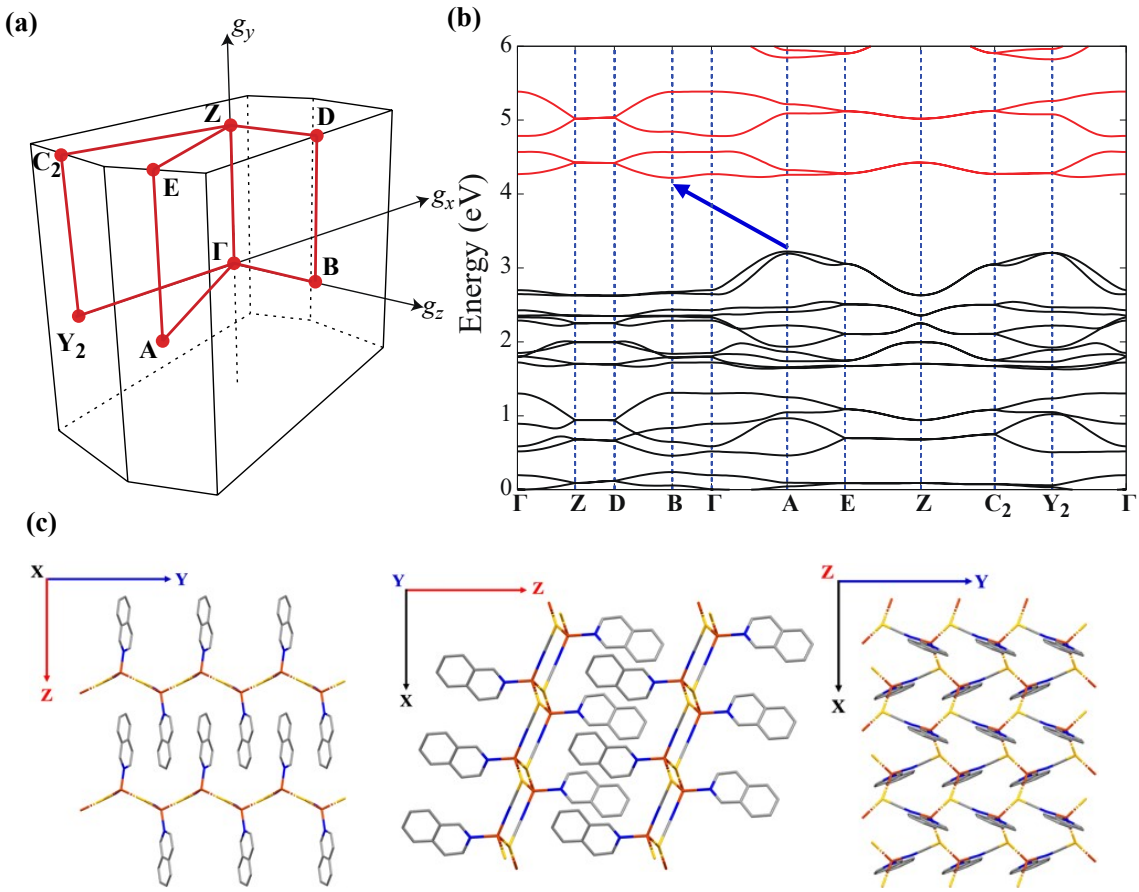

Fig. S10 (a) Brillouin zone of the crystal structure for $[Cu(SCN)iqi]_n$. The directions Γ−Z, Γ−Y_2, and Γ−B in the Brillouin zone correspond to the y-axis midle of (c), x-axis left of (c), and z-axis right of (c). (b)Band energy dispersion E(k) for $[Cu(SCN)(iqi)]_n$; blue arrows indicate the indirect bandgap (0.99 eV) at a bandgap between A and B points, respectively.

Calculations based on density functional theory (DFT) were carried out using the Vienna ab initio simulation program (Quantum ESPRESSO). The ion-core interactions were presented by the projector-augmented wave (PBE) method. The PBE exchange-correlation function developed by Perdew, Burke, and Ernzernhof was used with Grimme's D3 dispersion correction. The energy cutoff for the plane wave basis set was 90 rydberg was used. At first, geometrical optimizations with both atomic-coordinate and unit-cell relaxations were done using the standard DFT calculation with 6 × 6 × 6 Monkhorst-Pack k-point mesh for the Brillouin Zone integration was used. Next, we did the single-point SCF calculation with 8 × 8 × 8 Monkhorst-Pack k-point mesh for the subsequent electronic band-structure and projected density-of-state (PDOS) analyses. All

k-points in the Brillouin zone for the band structure calculations were determined by the SeeK-Path.[11], [12]

[1] CrysAlisPro: Data Collection and Processing Software, Rigaku Corporation (**2015**). Tokyo 196-8666, Japan.

[2] Dolomanov, O.V.; Bourhis, L.J.; Gildea, R.J.; Howard, J.A.K.; Puschmann, H., J. Appl. Cryst., **2009**, 42, 339-341.

[3] Sheldrick, G.M. Acta Cryst., **2015**, A71, 3-8.

[4] Sheldrick, G.M. Acta Cryst., **2015**, C71, 3-8.

[5] Lin, P.; Henderson, A. R.; Harrington, W. R.; Clegg, W.; Wu, C.; Wu, X. *Inorganic Chemistry*, **2004**, 43,

[6] Pilar Amo-Ochoa, Lorena, W.; Rodrigo, G. P.; Pablo, J. S. M.; Carlos, J. G.G.; Eva, M.M.; Salome D.; Julio, G. H.; Felix, Z. Chem. Commun., **2010**, 46, 3262–3264

[7] Tang, Z.; Weng, Y.; Yin, W.; Jiang, M.; Zhu, Q.; Dai, J. *Inorg. Chem.*, **2019**, 58, 15824−15831

[8] Okubo, T.; Himoto,K.; Tanishima, K.; Fukuda, S.; Noda,Y,; Nakayama, M.; Sugimoto, K.; Maekawa, M. Kuroda-Sowa, T. *Inorg. Chem*., **2018**, 57, 2373−2376

[9] Lei, S.; Christopher, H. H.; Sarah, S. P.; Yuri, T.; Ruomeng, W.: Fang, W.; Aron, W.; Mircea, D. *Chem. Sci*., **2017**, 8, 4450–4457

[10] Xiaofei, K.; Shanci, C.; Lingyi, M.; Jing, C.; Ting, H.; Xiaoyuan, W.; Guanhua, Z.; Guiming, Z.; Yuhang, L.; Can-Zhong, L. *Chem.Commun.,* **2019**, 55, 1643-1646

[11] Hinuma, Y.; Pizzi, G.; Kumagi, Y.; Oba, F.; Tanaka, I. *Comput. Mater. Sci.*, **2017**, 128,140-184

[12] Togo, A.; Tanaka, I.; *Spglib*: A software library for crystal symmetry search. *arXiv* **2018**, arXiv:1808.01590v1